Applied Environmental Research
- RESEARCH FOR SUSTAINABLE PLANET -

Research Article

Potential Factors of Landslide Recurrence in Uttaradit, Thailand: A Case Study in Laplae, Mueang Uttaradit, and Tha Pla Districts

Panithan Sawatdikomon[1], Watit Khokthong[2,3], Nipada Santha[1,*]

[1] *Department of Geological Sciences, Faculty of Science, Chiang Mai University, Chiang Mai, Thailand*
[2] *Environmental Science Research Center, Faculty of Science, Chiang Mai University, Chiang Mai, Thailand*
[3] *Department of Biology, Faculty of Science, Chiang Mai University, Chiang Mai, Thailand*

*Correspondence Email: nipada.santha@cmu.ac.th

Abstract

Laplae, Mueang Uttaradit, and Tha Pla district, Uttaradit province, Thailand are considered as high potential landslide areas. Still, this disaster is difficult to address because of complex factors controlling its occurrence. Therefore, the prediction of the potential landslide area using a landslide susceptibility map has been able to accomplish as a great strategy for the disaster. A landslide susceptibility map was produced by the geographic information system (GIS) data. The methods were initially conducted by the selection of potential factors related to landslides, which were lithology, slope, aspect, plan curvature, profile curvature, distance to stream, land use, and rainfall. All factors were assigned coefficients weight, and analyses frequency ratio (FR). Then, the weighted variables have been combined and ranked into five different susceptibility levels, which were very low, low, medium, high, and very high. Finally, the produced landslide susceptibility map has been validated by the success rate and prediction rate. After the analysis, the high and the very high landslide susceptibility area were dominantly covered in the northern and northwest parts of the study area; and the factor of slope, land use, and lithology potentially caused the landslide risk indicated by high frequency ratio values. In addition, the produced landslide susceptibility map had high accuracy, about 90% of success rate and prediction rate, calculated from the area under the curve (AUC), this map would be beneficial for geological hazard management and land use planning. The landslide susceptibility map and the GIS-based methods can be applied to the regional area with additional benefits to well-being, society, and the environment.

ARTICLE HISTORY

Received: 13 Feb. 2023
Accepted: 30 Jun. 2023
Published: 22 Sep. 2023

KEYWORDS

Frequency ratio;
Geographic information system;
Landslide;
Susceptibility map;
Uttaradit

Introduction

Climate change contributes to more disasters in the future since it relates to meteorological variability including precipitation, rainfall, temperature, wind speed, vegetation, and terrestrial alterations [1–3]. Especially, the latter alteration is a common consequence of natural processes; it is indeed vicious because of anthropogenic activities [4]. For example, a stream carves its channel during the wet season and then the change of land use from vegetation causes sudden alteration of drainage movements and exogenous earth's processes. Both factors contribute to the increasing of natural worldwide disasters, especially landslides. Landslide is one of the vital signs of vegetation and terrestrial alteration and it is a severe geological hazard [5] that occurred from a mass of rock, debris, or earth movement down a slope under the influence of gravity [6–7]. Landslides are an incalculable disaster because it was controlled by complex factors. This issue leads to difficulty in addressing and preventing [8-9]. To face the catastrophe, spatial assessment and landslides susceptibility are often preliminary evaluations to forecast the potential landslide [10], which is crucial in landslide risk management, policy supporting, and sustainable land use planning [11–12].

https://doi.org/10.35762/AER.2023016

Landslides have significant multi-dimensional impacts, including fatal damage, economic, social, and environmental impacts. In Thailand, landslides have recurrently occurred and they cover widespread more than fifty-two provinces, approximately more than 5 million rai [13]. From 1788 to 2007, there was reported that landslides killed more than 534 people and the estimated property damage was over 4,585.6 million Thai Baht [14]. To date, there are continuous reports that landslides had been recurring, yet the destruction had not been appraised. This mass wasting caused not only death and financial impacts, but also natural and environmental impacts, such as decreasing the number of vegetation areas and wildlife, unbalancing of ecosystems, drought problems, and soil erosion [15].

In Thailand, three districts in Uttaradit Province: Laplae, Mueang Uttaradit, and Tha Pla, can be considered as a crucial area in the northern part that affected by landslide disasters. This study area was found a great number of landslide scars or traces from the satellite images more than 9,000 scars, which is one potential landslide recurrence area [16]. This problem can be noticed in that landslide susceptibility maps are compulsory analyses for landslide prevention and risk mitigation.

Landslide susceptibility mapping has been proven to benefit from the development of computer-based technologies [1]. Especially, analyzing landslide risk can be assisted by the geographic information system (GIS) that is possible to detect sensitivity and accuracy based on model predictions in such landslide risk areas. Several models were taken into consideration using a large number of factors, which can include geomorphic [17] lithology [9] and anthropogenic elements [18] such as rock groups [19], physical slope aspects [9], risk map [10], local weather information [20], hydrographical networks [9], land use maps [21], and vegetation types [9]. The models of landslide risk can be verified using various techniques, for example, analytic hierarchy process (AHP), bivariate, multivariate, logistics, regression, fuzzy logic, or artificial neural network (ANN) [22]. Apart from these variables, the performance of the model can be evaluated using the FR and logistic regression methods to test analysis performance [23]. Thus, landslide susceptibility maps can be produced by many GIS-based models that will be utilized for landslide inventories and map creation in the future. Therefore, a plan to mitigate the effects of a probable landslide to find the potential factors of landslides.

The frequency ratio (FR) method is widely recognized as a reliable technique for landslide susceptibility mapping. Previous comparative studies consistently demonstrated the superior performance of the FR method. In a study conducted in Selangor State, Malaysia, different techniques, including FR and logistic regression model, were compared for landslide susceptibility mapping and this finding confirmed that higher accuracy of the FR method in estimating landslide area [24]. Similar to another study conducted in northwest Ethiopia for community-level landslide susceptibility mapping, the FR method was compared to the weight of evidence method that the former could produce more efficient and accurate landslide susceptibility maps than the weight of evidence method [25]. In Mae Phun, Uttaradit, Thailand, the FR method exhibited the highest prediction rate among the evaluated methods and this finding emphasized the effectiveness of the FR method in predicting landslide susceptibility [26].

This study aims to ensure the performance of FR in landslide susceptibility modeling at the local study and spot the potential risk of landslides where shallow landslides could occur in the future. To reach the objective, spatial information has been utilized to create the landslide susceptibility map in three districts of Uttaradit Province. Eight natural and anthropogenic factors have been selected, assigned the coefficients weight of each of the factors, and analyzed the FR. Then, the weighted variables have been combined and ranked into five different susceptibility levels. Finally, the resulting landslide susceptibility map has been validated by a success rate curve, prediction rate curve, and landslide density index, which also show the potential factors causing landslides.

Materials and methods

1) The study area

The study site covers the districts of Laplae, Mueang Uttaradit, and Tha Pla in Uttaradit Province, the northern part of Thailand (Figure 1). The area is approximately 2,580 km^2 or 33.0% of Uttaradit Province [27]. It bounds between 99° 53’ 48’’ E to 100° 46’ 46’’ E longitudes, and 17° 28’ 50’’ N to 18° 02’ 56’’ N latitudes. The elevation of the study area ranges from 400 to 1,000 m above mean sea level [27].

The area can be classified into three main regions, which are the watershed area, the narrow plain between valleys, and the hillside. The watershed area, which covers some parts of Laplae and Mueang Uttaradit district, spans across Nan River and its tributaries. The narrow plain between valleys is in the other parts of Laplae and Mueang Uttaradit Districts. The hillside area or the mountain range partly distributes in all three districts and the slope gradient ranges from 0° to 72°. These three districts had the numbers of population about 246,847 people [28]. In 2022, the average annual rainfall is 1,400 mm, specifically reaching 1,500 mm

during the rainy season [28]. The average temperature is from 15°C to 35°C [27].

2) Data processing

Landslide susceptibility map was created in ArcMap 10.8 software. Prior to processing, spatial data and landslide scar from Google Earth image are collected. All of factor data was converted into raster files, that were produced landslide susceptibility map using frequency ratio analysis from 80.0% of landslide inventory map (Google Earth image). Lastly, the model was validated by 20.0% of landslide inventory map using the area under the curve (AUC) and landslide density index. The flowchart of the research work is shown in Figure 2.

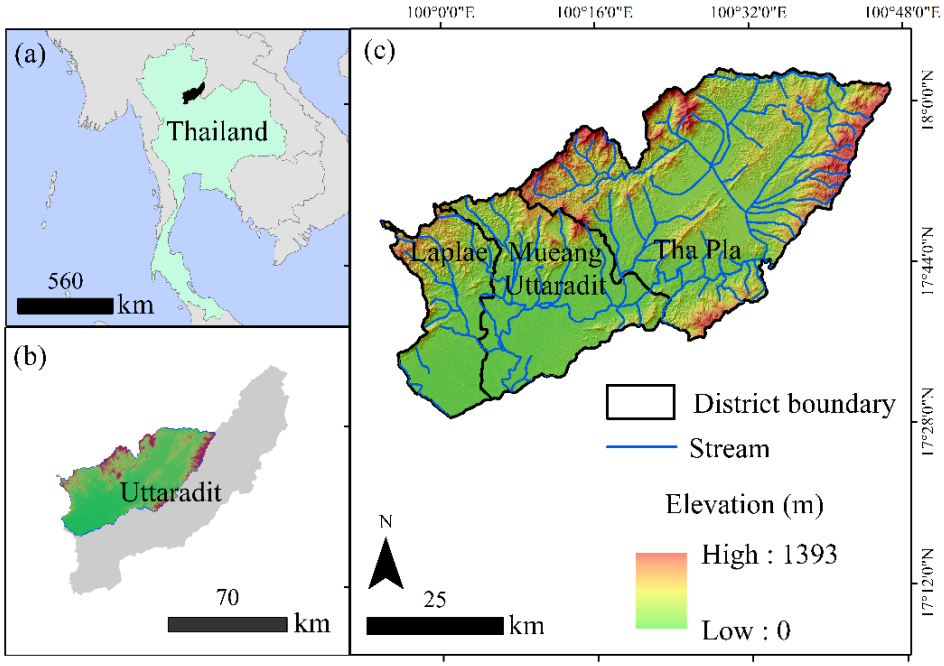

Figure 1 Pictures showing (a) the location of Uttaradit Province in Thailand, (b) Laplae, Mueang Uttaradit, and Tha Pla districts in Uttaradit Province and (c) the boundary of three districts with their elevation.

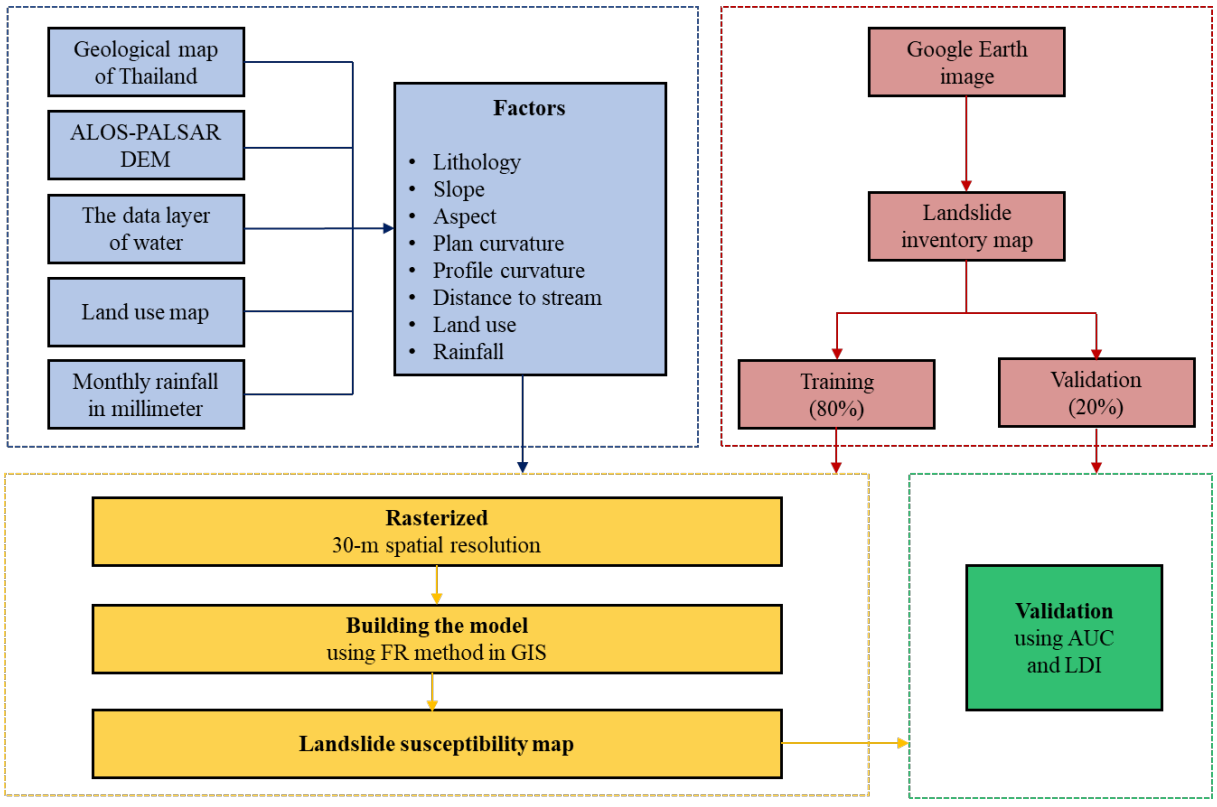

Figure 2 A schematic diagram of the research work.

2.1) Data collection and preparation

In this study, eight factors have been used, including lithology, slope, aspect, plan curvature, profile curvature, distance to stream, land use, and rainfall (Table 1). The input data for all factors were collected from various sources (Table 1).

The geological map of Thailand has a scale of 1:250,000 and it has shown nine lithological units namely granitic rocks, limestone-dominated rocks, fluvial deposits, terrace deposits, shale, slate, phyllite and schist, clastic rocks, ultramafic rocks, volcanic and tuffaceous rocks, and water bodies [29, 34–35] (Figure 3a). All rock units in shapefiles were rasterized to 30-m spatial resolution; however, the water bodies were excluded in the processing step.

Slope and aspect were produced using the Advanced Land Observing Satellite Phased Array Type L-band Synthetic Aperture Radar Digital Elevation Model (ALOS-PALSAR DEM) with 30-m spatial resolution. For the slope, the degrees were classified into five classes including 0°–5°, 5°–12°, 12°–30°, 30°–45° and more than 45° (Figure 3b) [30]. The aspect was divided into nine classes namely flat, which is defined as flat areas having no direction of downslope, north (337.5° –360°, 0°–22.5°), northeast (22.5°–67.5°), east (67.5°– 112.5°), southeast (112.5°–157.5°), south (157.5°–202.5°), southwest (202.5°–247.5°), west (247.5°–292.5°) and northwest (292.5°–337.5°) [25, 36–37] (Figure 3c).

The plan and profile curvature were also derived from ALOS-PALSAR DEM with 30-m spatial resolution, using the reclassify tool in ArcMap 10.8 [30, 38–39] (Figure 3d and 3e). The plan curvature was divided into three classes of curvature namely concave, flat, and convex, which have values of -32.850 to -0.001, -0.001 to 0.001, and 0.001 to 39.870, respectively. For the profile curvature was classed into three classes that represent three types of curvature: convex, flat, and concave (-58.690 to -0.001, -0.001 to 0.001, and 0.001 to 38.640, respectively).

For distance to stream, the shapefile of stream networks was analyzed by Euclidean distances in ArcMap 10.8. The buffer distance was classified into five classes (0–100, 100–200, 200–300, 300–400, 400–500, and more than 500 meters) [25, 31, 40–41] (Figure 3f), then it was rasterized with 30-m spatial resolution.

The land use map in level 2 was reclassified into six classes, namely agricultural areas, evergreen forests, other forest land areas, rangeland and miscellaneous areas, urban and built-up areas, and water bodies [26, 31, 39, 42] (Figure 3g). Then, all reclassified classes were rasterized into TIF format with 30-m spatial resolution.

The rainfall intensity map was generated using the inverse distance weighted (IDW) technique as one of the interpolation toolsets. The analysis incorporated data from nine rainfall stations, which are from Uttaradit, Phrae, Nan and Phitsanulok, and Sukhothai Provinces, Thailand: Tha Pla (Code 700151, N.12A, in Uttaradit), Tron (Code 700221, N.60, in Uttaradit), Mueang Phrae (Code 400013 in Phrae), Sung Men (Code 400022 in Phrae), Huai Rai Khao Phlung Forest Plantation (Code 400072 in Phrae), Den Chai (Code 400092 in Phrae), Na Muen (Code 280312 in Nan), Wat Bot (Code 390161, N.40, in Phitsanulok), and Si Satchanalai (Code 590121, Y.6, in Sukhothai). The natural breaks method was employed to divide the ranges of rainfall intensity into five classes: 1,112–1,149, 1,149–1,175, 1,175–1,201, 1,201–1,228, and 1,228–1,266 mm per year [25, 26, 33] (Figure 3h).

Table 1 The data sources of each factor

Input data	Sources (year)	Factors	Original formats
Geological map of Thailand (Scale 1:250,000)	Department of Mineral Resources (2015) [29]	Lithology	Vector (Shapefile)
ALOS-PALSAR DEM	Alaska Satellite Facility (2009) [30]	Slope, aspect, plan curvature, and profile curvature	Raster (TIFF, resolution 12.5 m)
The data layer of water	Department of Water Resources (2020) [31]	Distance to stream	Vector (Shapefile)
Land use map	Land Development Department (2018) [32]	Land use	Vector (Shapefile)
Monthly rainfall in millimeter	Royal Irrigation Department (2008-2018) [33]	Rainfall	Spreadsheet

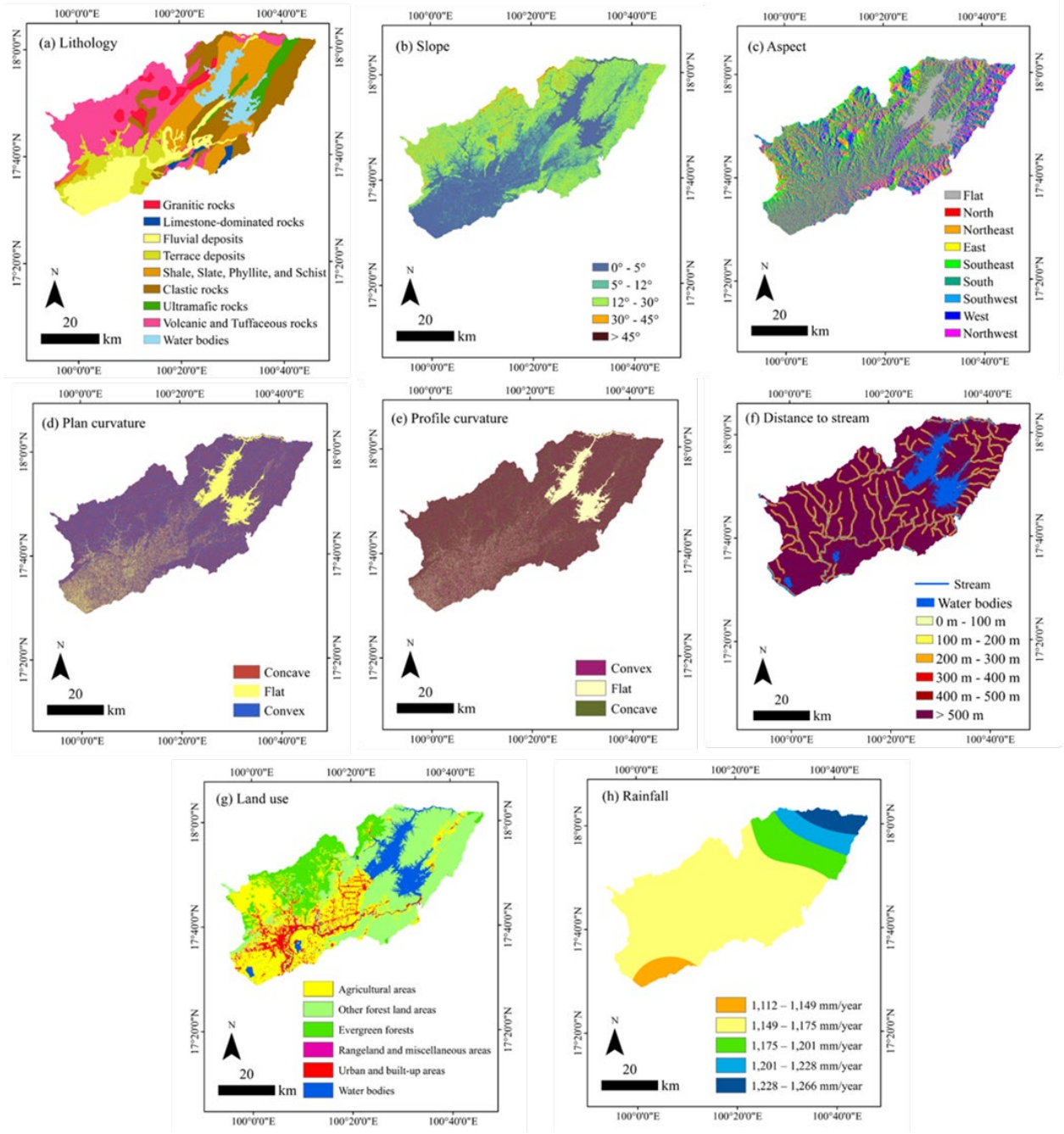

Figure 3 Input maps for landslide susceptibility model including (a) lithology, (b) slope, (c) aspect, (d) plan curvature, (e) profile curvature, (f) distance to stream, (g) land use, and (h) rainfall.

2.2) Preparation data from landslide inventory map

The inventory map of the landslide was used for training and validation processes. The landslide scars were carried out by Mineral Resources Region 1, Department of Mineral Resources, Thailand, using manually digitized based on the Google Earth imagery producing total of 10,204 polygons between 1984 and 2020 [43]. Afterward, the landslide inventory map was rasterized to 30-m spatial resolution. There was a total of 24,834 landslide pixels in the study area, which accounted for 22.350 km^2. For training and validation data, landslide pixels were randomly distributed. The data set of 20,151 landslide pixels (80.0%) was used as training and the other 4,683 landslide pixels (20.0%) were used as validation datasets (Figure 4).

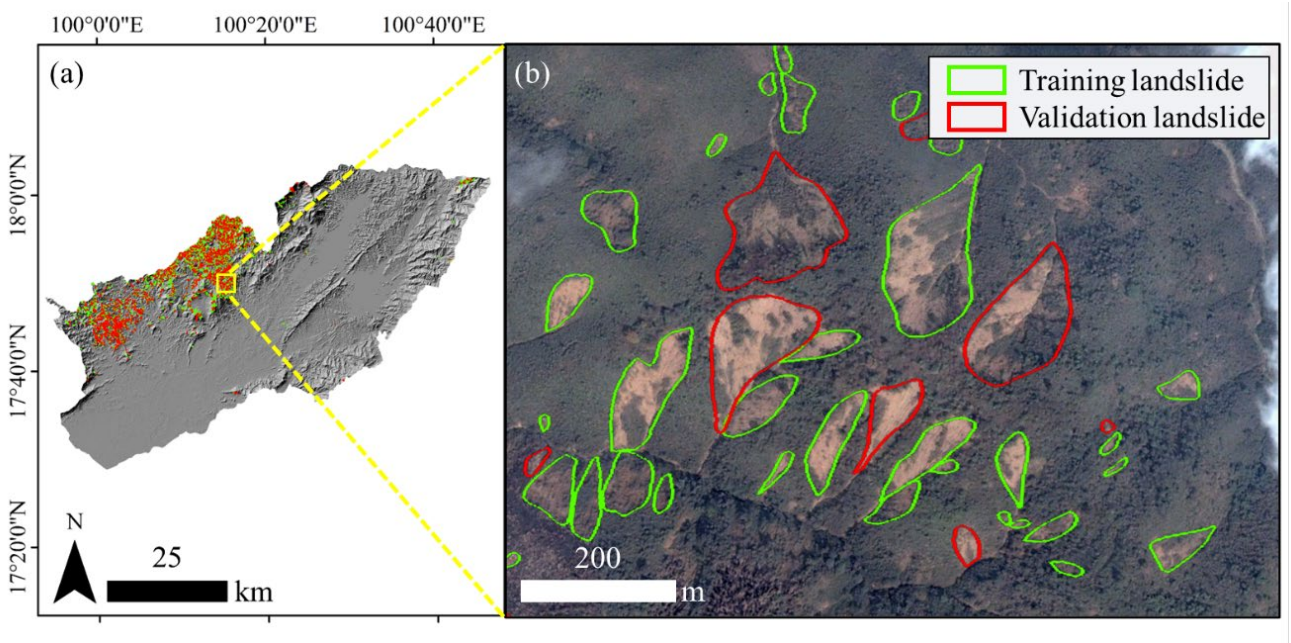

Figure 4 Pictures showing (a) all landslide scars in the study area and(b) example of polygons of landslide scars for validation and training.

2.3) Bivariate statistical analysis using frequency ration (FR)

To calculate the FR value of each factor for landslide susceptibility analysis, each thematic map was separately matched with the training datasets, and then the FR value was computed for each class in the ratio as Eq. 1 [25].

$$FR_i = \frac{NpixL_i \,/\, \Sigma NpixL_i}{NpixN_i \,/\, \Sigma NpixN_i} \qquad \text{(Eq. 1)}$$

Where FR_i is the frequency ratio value of each class of the causative factor; $NpixL_i$ is the number of landslide pixels in class i; $NpixL_i$ is the total number of landslide pixels in the study area; $NpixN_i$ is the number of pixels in class i; $NpixN_i$ is the total number of the study area.

If the FR_i value is more than 1, it indicates a high probability of landslide. There is a low probability when FR_i value is less than 1. If the FR_i value is equal to 1, there is a moderate chance of landslides [40]. The summation of FR values of all factors indicates landslide susceptibility index (LSI) as shown in Eq. 2 [25] that will be used to produce a landslide susceptibility map.

$$LSI = FR_1 + FR_2 + FR_3 + \ldots + FR_n \qquad \text{(Eq. 2)}$$

Where LSI is the landslide susceptibility index; FR is the frequency ratio value; n is the total number of causative factors used.

For the current study, the initial step was rasterized all the factors and landslide scars into raster format with 30-m spatial resolution. Then, landslide training datasets and all factors were used to compute the FR values of each factor class by the method of calculation in Eq. 1 [25]. Afterward, the FR value of each factor was summed by Eq. 2 [25] using the raster calculator of the spatial analyst tool in ArcMap 10.8 and the result of this process is the LSI map that was forward reclassified into five classes of landslide susceptibility ranking from very low, low, moderate, high, and very high.

3) Validation processes

3.1) Area under the curve (AUC)

The training landslide dataset (80.0%) and validation landslide dataset (20.0%) (from 2.2) were used for generation success rate curve and prediction rate curve, respectively. Landslide susceptibility index (LSI) values were divided into one-hundred classes by quantile reclassify method in ArcMap 10.8 and all class was sorted into descending order from high to low landslide susceptibility index. The training data (80.0%) was plotted with 100-classed landslide susceptibility index producing the AUC of success rate and the plotted graph between the validation data sets and landslide susceptibility index were calculated the AUC representing the prediction rate [26]. The success rate explains the capacity of landslide susceptibility model to reliably classify the occurrence of existing landslides and the prediction rate indicates the potential of the current landslide susceptibility model [44]. If the AUC value is lower than 50.00%, the model is rejected. The AUC values can be divided into 3 ranges; less than 70.0%, 70.0%–80.0%, and greater than 80.0% which represent sub-optimal performance, good performance, and excellent performance model respectively [45].

3.2) Landslide density index (LDI)

The validation landslide dataset (20.0%) which has not been used for building the model, can be considered as the future landslide area and was used to calculate LDI. Landslide density index is the ratio between the percentage of validation landslide pixels in each landslide susceptibility class and the percentage of each class pixel in the landslide susceptibility map. LDI can be calculated using the formulae in Eq. 3 [25].

$$\text{LDI} = \frac{\textit{percentage of validation landslide pixels}}{\textit{percentage of area pixel}} \quad \text{(Eq. 3)}$$

The suitability of any susceptibility map can be validated if a higher percentage of landslides occur in the high and very high susceptibility zones as compared to other zones.

Results and discussions

1) Frequency ratio (FR) values

The relationship between the probability of landslides and causative factors was examined by FR. The greater number of FR values indicates that factor supporting higher susceptibility of landslide occurrence; similarly, the small number of FR identifies as the high resistance for landslide susceptibility. The FR of all factors is in Table 2.

Considering each factor as shown in Table 2, the most significant factors are slope, land use, and lithology respectively. The largest number of FR is slope higher than 45°. The second and third important factors are other forest land areas (4.522), and lithology of volcanic and tuffaceous rock (3.091), respectively (Table 2).

In terms of land use, the agricultural areas have a lower FR value, while it is higher in other forest land areas (4.522) (Table 2). Although some previous studies found different consequences [37, 50] and they said that dense forests can protect the topsoil failure due to binding soil particles by plant root systems, but the forests as dense forests can impede runoff. Consequently, the runoffs permeated into soil pores that could result in increasing of water pressure and finally causes landslides [39, 42, 48, 51].

The third important factors, lithology shows that volcanic and tuffaceous rocks have the greatest number of FR (3.901), followed by granitic rocks (1.392), and clastic rock (0.943). The other categories of rock showed extremely low values that are less than 0.1 (Table 2). The influence of lithology on landslides is discussed in various ways and specific to the different study areas. The most favorable rocks, which tend to possess landslides, are volcanic and tuffaceous rocks (Table 2). The instability of volcanic and tuffaceous rocks was proved in the laboratory scale, and it was found that weathered volcanic tuffs produce clay minerals known as montmorillonite, which have a significant ability to swell and decrease of slope stability [52–53].

Moreover, our results suggest that slope has the most influence on the spatial distribution of landslides as well as each slope class considerably increases with the rising angle of slope gradient. This study correlated to other previous studies [25, 46], specifically one study of landslides susceptibility map in Mae Phun, Uttaradit, Thailand [26]; the research explained that shear stress of soil or other unconsolidated materials typically increases as the slope angle increases, indicating that high slope gradient is the important factor contributing to landslides [26]. However, there were some previous studies [47–49] argued that the slopes greater than 45° have a low landslide impact when the lithology is bedrock outcroppings or non-completely weathered rock. Therefore, lithology should be considered as a combination of the slope.

FR calculation of eight factors suggested that the landslides in the districts of Laplae, Mueang Uttaradit, and Tha Pla in Uttaradit Province, the northern part of Thailand significantly controlled by slope, land use (other forest land areas), and lithology. Indeed, the consideration among the three main factors (slope, land use, and lithology), it can explicit that some area exhibits slope greater than 30 degrees and exceeding 45°, but it shows a relatively low to moderate risk of landslides, since lithology is the presence of shale, slate, phyllite, and schist rock units, which exhibit an extremely low FR value of just 0.001. For instance, in Nang Phaya Subdistrict located at the northwestern the of Sirikit Dam, this case can be highlighted that although the slope has highest FR, a single factor may not always result to the good prediction. This could be from the combined factors in analysis of the landslide susceptibility map. Our study emphasizes that not only slope is the important factor, but also land use and lithology are the significant factors in this study area.

Table 2 Frequency ratio value in each factor class of the landslide causative factors

Factor and class	$NpixL_i$	% $NpixL_i$	$NpixN_i$	% $NpixN_i$	FR_i
Lithology					
Granitic rocks	1,036	5.14	123,052	3.69	1.392
Limestone-dominated rocks	8	0.04	35,258	1.06	0.038
Fluvial deposits	0	0.00	479,004	14.38	0.000
Terrace deposits	26	0.13	300,297	9.01	0.014
Shale, slate, phyllite and schist	2	0.01	593,560	17.81	0.001
Clastic rocks	3,582	17.78	628,293	18.86	0.943
Ultramafic rocks	62	0.31	120,898	3.63	0.085
Volcanic and tuffaceous rocks	15,435	76.60	825,719	24.78	3.091
Water area	0	0.00	226,033	6.78	0.000
Slope (degree)					
0–5	164	0.81	1,199,526	36.00	0.023
5–12	1,092	5.42	703,796	21.12	0.257
12–30	11,374	56.44	1,295,889	38.89	1.451
30–45	7,236	35.91	130,415	3.91	9.175
> 45	285	1.41	2,488	0.07	18.942
Aspect					
Flat	35	0.17	259,165	7.78	0.022
North	2,028	10.06	325,027	9.75	1.032
Northeast	3,362	16.68	358,599	10.76	1.550
East	3,234	16.05	373,241	11.20	1.433
Southeast	3,320	16.48	417,538	12.53	1.315
South	2,284	11.33	406,086	12.19	0.930
Southwest	2,492	12.37	420,810	12.63	0.979
West	2,043	10.14	393,700	11.82	0.858
Northwest	1,353	6.71	377,948	11.34	0.592
Plan curvature					
Concave	10,767	53.43	1,271,349	40.59	1.316
Flat	99	0.49	487,905	15.58	0.032
Convex	9,285	46.08	1,372,860	43.83	1.051
Profile curvature					
Convex	9,895	49.10	1,322,097	42.21	1.163
Flat	84	0.42	363,649	11.61	0.036
Concave	10,172	50.48	1,446,368	46.18	1.093
Distance to stream (m)					
0–100	537	2.66	195,723	5.87	0.454
100–200	576	2.86	193,034	5.79	0.493
200–300	748	3.71	189,571	5.69	0.652
300–400	794	3.94	186,709	5.60	0.703
400–500	925	4.59	182,623	5.48	0.838
> 500	16,571	82.23	2,384,454	71.56	1.149
Land use					
Agricultural areas	5,427	26.93	1,065,643	31.98	0.842
Evergreen forests	799	3.97	1,202,970	36.10	0.110
Other forest land areas	13,908	69.02	508,535	15.26	4.522
Rangeland and miscellaneous areas	0	0.00	38,605	1.16	0.000
Urban and built-up areas	2	0.01	183,111	5.50	0.002
Water bodies	15	0.07	333,250	10.00	0.007
Annual rainfall (mm)					
1,112–1,149	0	0.00	133,318	4.00	0.000
1,149–1,175	19,561	97.07	2,441,096	73.26	1.325
1,175–1,201	136	0.67	400,060	12.01	0.056
1,201–1,228	2	0.01	204,151	6.13	0.002
1,228–1,266	452	2.24	153,489	4.61	0.487

Remark: $NpixL_i$ is the number of landslide pixels in class, $\%NpixL_i$ is the percentage of landslide pixels in class, $NpixN_i$ is the number of pixels in class, and $\%NpixN_i$ is the percentage of landslide in class.

2) Landslide susceptibility index (LSI) and landslides susceptibility classes

The FR value of each selected factor class was combined to develop the LSI map. The LSI values ranged from 0.567 to 32.878 (Figure 5), and they were reclassified by the natural breaks method. The results of LSI values presented five susceptibility classes: very low (0.567–7.409), low (7.409–11.717), moderate (11.717–17.293), high (17.293–25.782), and very high (25.782–32.878) (Figure 6). Besides, the percentage of area values

presented in five susceptibility classes: very low (9.03%), low (32.17%), moderate (30.85%), high (17.25%), and very high (10.71%), respectively (Table 3). The high and very high susceptibility classes, which should be in high inspection, were covered in the northern and north-western parts (Figure 6).

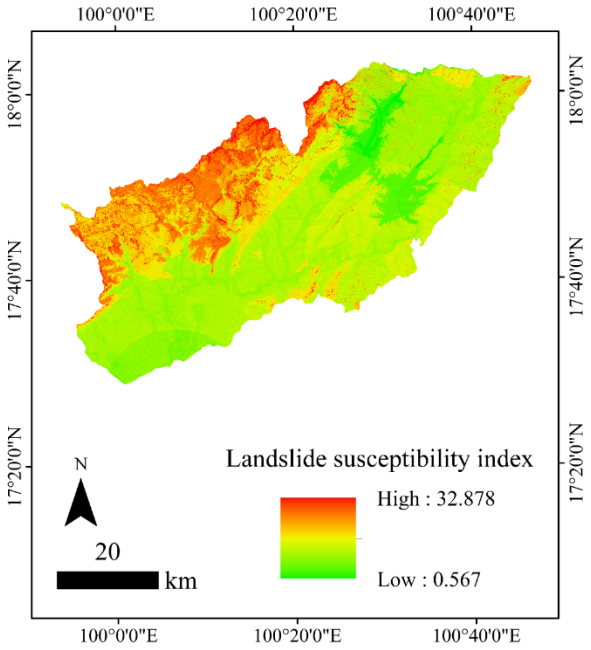

Figure 5 Landslide susceptibility index map of the study area using frequency ratio.

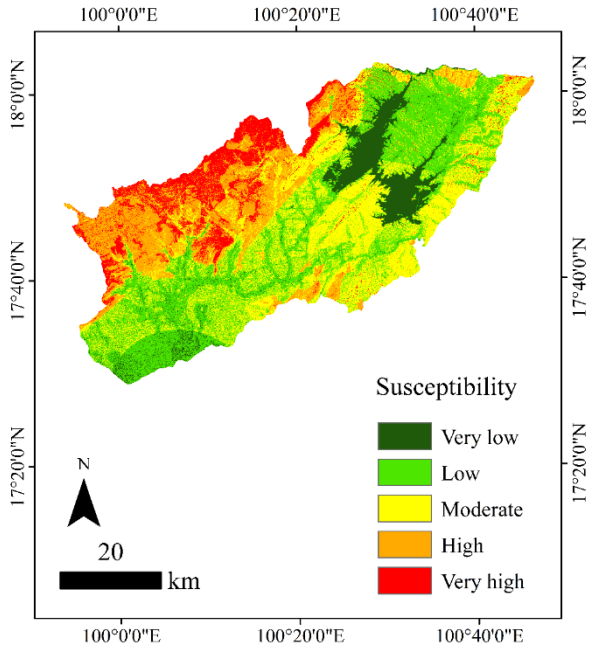

Figure 6 Landslide susceptibility map of the study area using frequency ratio.

These areas dominantly were high and very high risk, and they can be highlighted as more vulnerable because the landslide susceptibility map in high and very high risk can contribute to disaster planning.

3) Validation of the model

3.1) Area under the curve (AUC)

Model validation is an essential procedure to validate the landslide susceptibility maps. In this study, the landslide susceptibility maps evaluated the performance of the model using area under the curve of the prediction rate curve and the success rate curve [46]. The AUC of the prediction rate curve was produced by plotting the cumulative landslide susceptibility index values of all pixels on the x-axis and the cumulative validation landslide dataset (20.0%) on the y-axis. While the AUC of the success rate curve was plotted between the landslide susceptibility index values of all pixels the cumulative training landslide dataset (80.0%) was plotted on the y-axis instead. Regarding FR, the model using the bivariate statistical method has a high quality [25, 26, 54–56]. As can be seen in Figure 7a, the AUC value for the success rate was found at 90.3% and the prediction rate was found at 90.1% (Figure 7b) suggesting high performances of the landslide susceptibility model. The FR model can be applied to various sizes of area, including small areas covering from 100 to 997 km^2 with 77.8%–80.8% of AUC of prediction rate values [26], and large areas covering from 1,900 to 12,050 km^2 with 80.0%–87.3% of the area under the curve value [47, 49, 57]. In our case, the study covers 2,983.210 km^2 showing the highest area under the curve of the prediction rate, which is 90.1%.

3.2) Landslide density index (LDI)

Aside from the area under the curve of the success rate and prediction rate curves that are representative of overall simulation performance, the landslide density index is also one of the validation tests linking the consistency of the model. The landslide susceptibility model is valid when the LDI increases from very low to very high classes [46]. The LDI from the validation (64.2%, Table 3) showed that the very high susceptibility class was the majority of the landslide distribution followed by high, moderate, low, and very low, respectively. Besides, 63.9% for the training landslide dataset also shows the same pattern as the validated LDI. The LDI value for very high susceptibility class was 6.000 which is remarkably higher than the other classes (Table 3). This behavior is the same as that observed in the performed experiments [34, 58–61] that landslide density index increases from very low to very high class, but previous research gained the landslide density index value in the highest susceptibility class about 80.0%–87.3%; whereas, our study was found the prediction rate at 90.1% (Figure 7b). The results indicate that the landslide susceptibility map produced from the frequency ratio analysis is reliable.

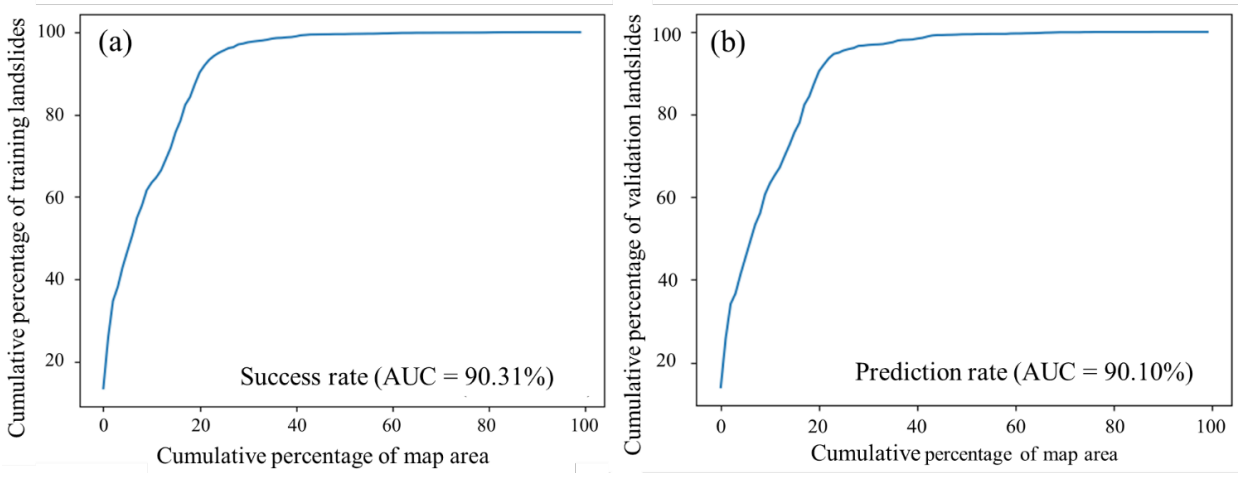

Figure 7 Plots of (a) area under the curves of success rate and (b) area under the curves of prediction rate curves.

Table 3 The relation between landslide susceptibility class and landslide density index (LDI)

Landslide susceptibility class	Validation landslide pixels		Area pixels		Area (km^2)	LDI
	Number	%	Number	%		
Very low	0	0.00	299,220	9.03	269.300	0.000
Low	19	0.41	1,066,242	32.17	959.620	0.013
Moderate	140	2.99	1,022,581	30.85	920.320	0.097
High	1,515	32.37	571,767	17.25	514.590	1.877
Very high	3,006	64.23	354,865	10.71	319.380	6.000
Total	4,680	100.00	3,314,675	100.00	2,983.210	

As it can be noticed from high rank of AUC and LDI, this research has confirmed the reliability of landslides susceptibility maps using the databases and factual landslide scar maps.

3.3) Application of landslide susceptibility map and model

It is beneficial for residents to understand the most updated landslide susceptibility map. Especially in a high-risk landslide area, the organization can make plans to transfer knowledge about geohazard management and prevention. In this way, the updated or different landslide susceptibility models can be used for planning on bigger scales. For example, in a landslide-prone area, policymakers should limit in village settlement area to mitigate the landslide risk. Moreover, local governments or organizations can use the updated landslide susceptibility map to install observation devices and warning systems, prepare evacuation plans and build emergency assembly points. Furthermore, the model of landslides can help with sustainable forest management showing some parts of forest areas are vulnerable where landslides potentially occur. This can make plans to conserve that forest site and recover that forest area in a time when landslides happen.

Conclusion

The landslide risk is currently interpreted based on basic GIS and map data. The landslide analysis gains the advantage of receiving reliable data. In this case, the landslide susceptibility map was already validated and showed very high landslide occurrences in the study site areas that could cause disaster in the future. The methods used in this research can be applied on a regional scale, especially in the northern part of Thailand or Laos. Still, the effectiveness of the results must be tested in the local communities. Fortunately, local organizations and related governmental departments could use this landslide susceptibility map for further implementation since this data could promote people's well-being as in the sustainable development goals (SDGs).

Acknowledgement

This research was supported by CMU Junior Research Fellowship Program, and, Chiang Mai University, Thailand. Authors would also like to acknowledge for the satellite images of landslide scars from Bureau of Mineral Resources Office Region 1 (Lampang), Ministry of Natural Resources and Environment, Thailand.

References

[1] Ageenko, A., Hansen, L.C., Lyng, K.L., Bodum, L., Arsanjani, J.J. Landslide susceptibility mapping using machine learning: A Danish case study. ISPRS International Journal of Geo-Information, 2022, 11(6), 324.

[2] Crozier, M.J. Deciphering the effect of climate change on landslide activity: A review. Geomorphology, 2010, 124(3–4), 260–267.
[3] Field, C.B., Barros, V., Stocker, T.F., Dahe, Q. Managing the risks of extreme events and disasters to advance climate change adaptation: special report of the intergovernmental panel on climate change. Cambridge University Press, 2012.
[4] Vitousek, P.M., Mooney, H.A., Lubchenco, J., Melillo, J.M. Human domination of Earth's ecosystems. Science, 1997, 277(5325), 494–499.
[5] Parise, M., Jibson, R.W. A seismic landslide susceptibility rating of geologic units based on analysis of characteristics of landslides triggered by the 17 January, 1994 Northridge, California earthquake. Engineering Geology, 2000, 58(3–4), 251–270.
[6] Creden, D.M. A simple definition of a landslide. Bulletin of the International Association of Engineering Geology, 1991, 43(1), 27–29.
[7] Varnes, D.J. Landslide hazard zonation: a review of principles and practice, 1984.
[8] Froude, M.J., Petley, D.N. Global fatal landslide occurrence from 2004 to 2016. Natural Hazards and Earth System Sciences, 2018, 18(8), 2161–2181.
[9] Roccati, A., Paliaga, G., Luino, F., Faccini, F., Turconi, L. GIS-based landslide susceptibility mapping for land use planning and risk assessment. Land, 2021, 10(2), 162.
[10] Pellicani, R., Argentiero, I., Spilotro, G. GIS-based predictive models for regional-scale landslide susceptibility assessment and risk mapping along road corridors. Geomatics, Natural Hazards and Risk, 2017, 8(2), 1012–1033.
[11] Corominas, J., Van Westen, C., Frattini, P., Cascini, L, Malet, J.P., Fotopoulou, S., Catani, F., Van Den Eeckhaut, M., Mavrouli, O., Agliardi, F., Pitilakis, K. Recommendations for the quantitative analysis of landslide risk. Bulletin of Engineering Geology and the Environment, 2014, 73, 209–263.
[12] Dai, F.C., Lee, C.F., Ngai, Y.Y. Landslide risk assessment and management: An overview. Engineering Geology, 2002, 64(1), 65–87.
[13] Department of Mineral Resources, Thailand. General information of geohazard: Landslide. 2022. [Online]. Available from: https://www.dmr.go.th [Accessed 12 March 2022].
[14] Department of Water Resources, Thailand. Risky factors and community living in landslide with flood areas or landslide areas: A case study of the northern part of Ping watershed. Bangkok: Kurusapa Printing Ladphrao, 2008. [Online] Available from: https://dwr.go.th/uploads/file/article/2018/article_th-05022018-102205-770150.pdf [Accessed 10 January 2022].
[15] Department of Mineral Resources, Thailand. Report of landslide risk in local area, 2022. [Online]. Available from: https://data.go.th/ dataset/gdpublish-landslide_report/. [Accessed 12 January 2022].
[16] Ruansorn, T. The study of contributed Landslide inventory in Uttaradit province by interpreting Google Earth satellite images. GEOTHAI 2021, Virtual Conference, Department of Mineral Resources, Online Conference. 2 August 2021.
[17] Cendrero, A.N., Remondo, J.U., Bonachea, J.A., Rivas, V., Soto, J. Sensitivity of landscape evolution and geomorphic processes to direct and indirect human influence. Geografia Fisica e Dinamica Quaternaria, 2006, 29(2), 125–137.
[18] Persichillo, M.G., Bordoni, M., Cavalli, M., Crema, S., Meisina, C. The role of human activities on sediment connectivity of shallow landslides. Catena, 2018, 160, 261–274.
[19] Soralumb, S. Corporative of geotechnical approach for landslide susceptibility mapping in Thailand. Geothechnique and Geosynthetics for Slopes. Chiangmai, Thailand, 2010, 1–8.
[20] Szaby, J. The relationship between landslide activity and weather: examples from Hungary. Natural Hazards and Earth System Sciences, 2003, 3(1/2), 43–52.
[21] Galve, J.P., Cevasco, A., Brandolini, P., Soldati, M. Assessment of shallow landslide risk mitigation measures based on land use planning through probabilistic modelling. Landslides, 2015,12, 101–114.
[22] Intarawichian, N., Dasananda, S. Analytical hierarchy process for landslide susceptibility in lower Mea Chaem watershed, northern Thailand. Suranaree Journal of Science & Technology, 2010, 17(3).
[23] Oh, H.J., Lee, S., Chotikasathien, W., Kim, C.H., Kwon, J.H. Predictive landslide susceptibility mapping using spatial information in the Pechabun area of Thailand. Environmental Geology, 2009, 57, 641-651.
[24] Lee, S., Pradhan, B. Landslide hazard mapping at Selangor, Malaysia using frequency ratio and logistic regression models. Landslides, 2007, 4(1), 33–41.
[25] Mersha, T., Meten, M. GIS-based landslide susceptibility mapping and assessment using bivariate statistical methods in Simada area, northwestern Ethiopia. Geoenvironmental Disasters, 2020, 7(1), 1–22.

[26] Moazzam, M.F., Vansarochana, A., Boonyanuphap, J., Choosumrong, S., Rahman, G., Djueyep, G.P. Spatio-statistical comparative approaches for landslide susceptibility modeling: case of Mae Phun, Uttaradit province, Thailand. SN Applied Sciences, 2020, 2, 1–5.

[27] Department of Mineral Resources, Thailand. Geology of Thailand. 2nd edition. Bangkok: Department of Mineral Resources, Thailand, 2007.

[28] Uttaradit Province Government, Thailand. General characteristics of Uttaradit province, 2022. [Online]. Available from: https:// www2.uttaradit.go.th/content/general_en [Accessed 12 January 2022].

[29] Department of Mineral Resources, Thailand. Geological map of Thailand scale 1:250,000. Thailand: Department of Mineral Resources, Thailand, 2015.

[30] Alaska Satellite Facility, JAXA/METI ALOS PALSAR L1.0 2009, 2009. [Online]. Available from: https://asf.alaska.edu [Accessed 14 January 2022].

[31] Department of Water Resources, Thailand. The data layer of water (FGDS) Department of Water Resources, 2020. [Online]. Available from: https://dataportal.asia/en/dataset/202661945_item_60fac91a-01c5-43da-b429-19e145a1ce7a [Accessed 12 January 2022].

[32] Land Development Department, Thailand. Land use map of Uttaradit province scale 1:25,000, 2018. [Online]. Available from: https://dinonline.ldd.go.th [Accessed 12 January 2022].

[33] Royal Irrigation Department, Thailand. Upper northern region irrigation hydrology center: Rainfall data, 2018. [Online]. Available from: https://www.hydro-1.net/main/3-RAIN.php [Accessed 12 January 2022].

[34] Akkrawintawong, K. Landslide hazard investigation in Changwat Nan. Doctoral dissertation, Chulalongkorn University, 2008.

[35] Yu, X., Zhang, K., Song, Y., Jiang, W., Zhou, J. Study on landslide susceptibility mapping based on rock–soil characteristic factors. Scientific Reports, 2021, 11(1), 1–27.

[36] Tseng, C.M., Lin, C.W., Hsieh, W.D. Landslide susceptibility analysis by means of event-based multi-temporal landslide inventories. Natural Hazards and Earth System Sciences Discussions, 2015, 3(2), 1137–1173.

[37] Khan, H., Shafique, M., Khan, M.A., Bacha, M.A., Shah, S.U., Calligaris, C. Landslide susceptibility assessment using frequency ratio, a case study of northern Pakistan. The Egyptian Journal of Remote Sensing and Space Science, 2019, 22(1), 11–24.

[38] Nefeslioglu, H.A., Sezer, E.B., Gokceoglu, C., Bozkir, A.S., Duman, T.Y. Assessment of landslide susceptibility by decision trees in the metropolitan area of Istanbul, Turkey. Mathematical Problems in Engineering, 2010, 2010.

[39] Javier, D.N., Kumar, L. Frequencet ration landslide susceptibility estimation in a tropical mountain region. International Archives of the Photogrammetry, Remote Sensing & Spatial Information Sciences, 2019.

[40] Lee, S., Talib, J.A. Probabilistic landslide susceptibility and factor effect analysis. Environmental Geology, 2005, 47, 982–990.

[41] Pourghasemi, H.R., Pradhan, B., Gokceoglu, C., Mohammadi, M., Moradi, H.R. Application of weights-of-evidence and certainty factor models and their comparison in landslide susceptibility mapping at Haraz watershed, Iran. Arabian Journal of Geosciences, 2013, 6, 2351–2365.

[42] Teerarungsigul, S., Torizin, J., Fuchs, M., Kьhn, F., Chonglakmani, C. An integrative approach for regional landslide susceptibility assessment using weight of evidence method: a case study of Yom River Basin, Phrae province, northern Thailand. Landslides, 2016, 13, 1151–1165.

[43] Department of Mineral Resources, Ministry of natural resources and environment. landslide susceptibility map in local scale, Uttaradit Province. Bangkok: Department of Mineral Resources, Thailand, 2021.

[44] Sadisun, I.A., Arifianti, Y. Weights of evidence method for landslide susceptibility mapping in Takengon, Central Aceh, Indonesia. In IOP Conference Series: Earth and Environmental Science, 2018.

[45] Draelos, R. Measuring Performance: AUC (AUROC). GLASS BOX, 2019. [Online] Available from: https://glassboxmedicine.com/2019/02/23/measuring-performance-auc-auroc/ [Accessed 2 January 2023].

[46] Getachew, N., Meten, M. Weights of evidence modeling for landslide susceptibility mapping of Kabi-Gebro locality, Gundomeskel area, central Ethiopia. Geoenvironmental Disasters, 2021, 8(1), 1–22.

[47] Mohammady, M., Pourghasemi, H.R., Pradhan, B., Landslide susceptibility mapping at Golestan Province, Iran: a comparison between frequency ratio, Dempster–Shafer, and weights-of-evidence models. Journal of Asian Earth Sciences, 2012, 61, 221–236.

[48] Ozdemir, A., Altural, T. A comparative study of frequency ratio, weights of evidence and logistic regression methods for landslide susceptibility mapping: Sultan mountains, SW Turkey. Journal of Asian Earth Sciences. 2013, 64, 180–197.

[49] Intarawichian, N., Dasananda, S. Frequency ratio model based landslide susceptibility mapping in lower Mae Chaem watershed, northern Thailand. Environmental Earth Sciences, 2011, 64, 2271–2285.

[50] Sarkar, S., Roy, A.K., Martha, T.R. Landslide susceptibility assessment using information value method in parts of the Darjeeling Himalayas. Journal of the Geological Society of India, 2013, 82, 351–362.

[51] Dai, F.C., Lee, C.F., Li, J.X., Xu, Z.W. Assessment of landslide susceptibility on the natural terrain of Lantau island, Hong Kong. Environmental Geology, 2001, 40, 381–391.

[52] Fall, M., Azzam, R., Noubactep, C. A multi-method approach to study the stability of natural slopes and landslide susceptibility mapping. Engineering Geology, 2006, 82(4), 241–263.

[53] Ayalew, L., Yamagishi, H. The application of GIS-based logistic regression for landslide susceptibility mapping in the Kakuda-Yahiko mountains, Central Japan. Geomorphology, 2005, 65(1–2), 15–31.

[54] Chen, W., Chai, H., Sun, X., Wang, Q., Din,g X., Hong, H. A GIS-based comparative study of frequency ratio, statistical index and weights-of-evidence models in landslide susceptibility mapping. Arabian Journal of Geosciences, 2016, 9, 1–6.

[55] Razavizadeh, S., Solaimani, K., Massironi, M., Kavian, A. Mapping landslide susceptibility with frequency ratio, statistical index, and weights of evidence models: a case study in northern Iran. Environmental Earth Sciences, 2017, 76, 1–6.

[56] Wang, L.J., Guo, M., Sawada, K., Lin, J., Zhang, J. A comparative study of landslide susceptibility maps using logistic regression, frequency ratio, decision tree, weights of evidence and artificial neural network. Geosciences Journal, 2016, 20, 117–136.

[57] Silalahi, F.E., Arifianti, Y., Hidayat, F. Landslide susceptibility assessment using frequency ratio model in Bogor, West Java, Indonesia. Geoscience Letters, 2019, 6(1), 1–7.

[58] Bijukchhen, S.M., Kayastha, P., Dhital, M.R. A comparative evaluation of heuristic and bivariate statistical modelling for landslide susceptibility mappings in Ghurmi–Dhad Khola, east Nepal. Arabian Journal of Geosciences, 2013, 6, 2727–2743.

[59] Wei, X., Zhang, L., Lu,o J., Liu, D. A hybrid framework integrating physical model and convolutional neural network for regional landslide susceptibility mapping. Natural Hazards, 2021 109, 471–497.

[60] Wubalem, A., Meten, M. Landslide susceptibility mapping using information value and logistic regression models in Goncha Siso Eneses area, northwestern Ethiopia. SN Applied Sciences, 2020, 2, 1–9.

[61] Fayez, L., Pazhman, D., Pham, B.T., Dholakia, M.B., Solanki, H.A., Khalid, M., Prakash, I. Application of frequency ratio model for the development of landslide susceptibility mapping at part of Uttarakhand State, India. International Journal of Applied Engineering Research, 2018, 13(9), 6846–6854.